

Molecular mechanics and molecular dynamics simulations of the hexagonal crystalline form of the helical polyamide poly(α -isobutyl-L-aspartate)

Carlos Alemán*, Jordi Bella† and Juan J. Perez

Departament d'Enginyeria Química, Escola Tècnica Superior d'Enginyers Industrials, Universitat Politècnica de Catalunya, Avinguda Diagonal 647, Barcelona E-08028, Spain (Received 19 February 1993; revised 3 November 1993)

The program AMBER 3.0 Rev.A has been used in a molecular mechanical study of two conformational models for the title compound on a simplified solid-state model with hexagonal coordination. Results show that the right-handed model is the minimum energy structure with a relative stability of 20 kcal mol⁻¹ residue. Molecular dynamics trajectories show less torsion angle variability in the backbone than in the side chain, according to the packing environment of each residue.

(Keywords: poly(α -isobutyl-L-aspartate); molecular mechanics; molecular dynamics)

INTRODUCTION

The helical structures¹ for the hexagonal and tetragonal^{2,3} crystalline forms of poly(α -isobutyl-L-aspartate) (PAIBLA; *Figure 1*) were discussed in earlier papers^{3,4}. Both X-ray diffraction analysis with the linked-atom least-squares (LALS) methodology⁵ and energy minimization calculations showed a right-handed helix for the tetragonal form⁴. On the other hand, LALS results indicate that there are two conformations, **1L** and **2R** (see *Figure 2*) (where **L** and **R** refer to a left-handed and a right-handed helix, respectively), compatible with the hexagonal form of PAIBLA⁴. Both models are consistent with the 13/4 helix (13 residues in four turns) observed experimentally³. In addition, theoretical calculations of the circular dichroism spectrum do not provide a distinction between them⁶. Preliminary energy minimization calculations favoured the model **2R**⁴. Nevertheless, these energy calculations were performed on an isolated chain, and consequently intermolecular side-chain interactions were not taken into account. In view of the importance of packing interactions in the structure of a crystalline polymer chain⁷⁻¹², these results could not be considered as definitive. In the present work we have analysed the conformational and potential energies of models **1L** and **2R**, considering both intramolecular and intermolecular interactions simultaneously within each minimization cycle, in order to ascertain which model is energetically favoured in the hexagonal crystalline form.

Moreover, in previous LALS calculations^{3,4} all side-chain groups were considered with the same conformation owing to the small number of diffraction spots available.

This is physically unreasonable in the hexagonal form, since depending on the packing environment the side chains could have different conformations. Thus, in order to investigate the conformational preferences of the side chains we performed a 60 ps molecular dynamics trajectory.

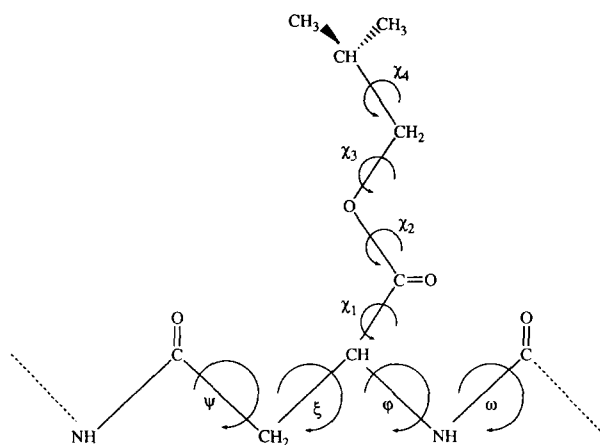


Figure 1 Schematic representation of a monomeric unit. The torsional angles are indicated. The amide group is repeated at both ends

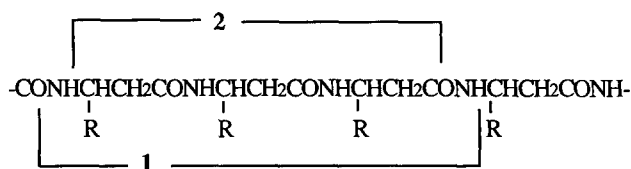


Figure 2 Different hydrogen-bonding schemes compatible with the hexagonal crystalline form conformations of poly(α -isobutyl-L-aspartate)

*To whom correspondence should be addressed

†Present address: Department of Chemistry, Rutgers, The State University of New Jersey, Piscataway, NJ 08855, USA

METHODS

All the calculations have been performed with explicit consideration of all atoms involved¹³ using the AMBER 3.0 Rev.A program^{14,15}. Potential energy parameters obtained elsewhere⁴ by quantum mechanical calculations^{16,17} were used.

Geometry optimizations were carried out in several steps. First, the starting conformations were subject to 250 cycles of steepest descent optimization to eliminate the worst steric conflicts. Second, subsequent optimization using a conjugate gradient algorithm was performed. All the structures were minimized until the difference in energy between two successive iterations was less than 10^{-7} kcal mol⁻¹ (1 cal = 4.2 J) or the norm of the gradient for two successive steps in the minimization was less than 0.1 kcal mol⁻¹ Å⁻¹‡.

Minimizations were carried out without any symmetry constraints. We imposed an 8 Å cut-off for the non-bonded interactions¹⁸, and updated the list of these interactions every 25 steps. Dielectric constants of $\epsilon=1$ and $\epsilon=1r$ provide the most reliable results in crystalline polymer systems⁷, and therefore both expressions were used in the energy optimization calculations.

In the molecular dynamics simulation a time step of 1 fs was used. The dielectric constant was fixed at $\epsilon=1r$. During the first 10 ps, the system was heated from 0 K to 298 K. The simulation was continued for 50 ps at 298 K. The results were averaged over the last 25 ps of the run. A configuration was stored every 1 ps for analysis.

RESULTS AND DISCUSSION

We used the coordinates obtained from the LALS analysis performed elsewhere⁴ to generate a polymer chain of 17 residues, which was blocked at the amino terminal end with an acetyl group and with an *N*-methylamide at the carboxy end. A simplified model of the hexagonal crystal form was mimicked by a central polymer chain surrounded by six equivalent chains (see Figure 3). In order to avoid end effects on the conformation, only the seven middle residues of the central chain were considered when analysing the conformation and, in addition, their dihedral angles were averaged. On the other hand, energy contributions were computed for the middle residue of the central chain¹. The results obtained from the energy minimization of models **1L** and **2R** appear in Table 1 and Figure 3.

As can be seen, the energy-minimized conformations are not drastically sensitive to the dielectric constant considered. Thus, both expressions, $\epsilon=1$ and $\epsilon=1r$, provide very similar conformations within each model. The small divergence of the minimized structures from those obtained from X-ray data refinement suggests that the original LALS conformations⁴ are reasonably accurate and very close to an energy minimum, in particular the model **2R** structure. Moreover, the peptide bond displays more reasonable values than those obtained from previous calculations on an isolated chain⁴. Thus, a very small deviation from planarity is observed in the peptide bond of **1L** when packing

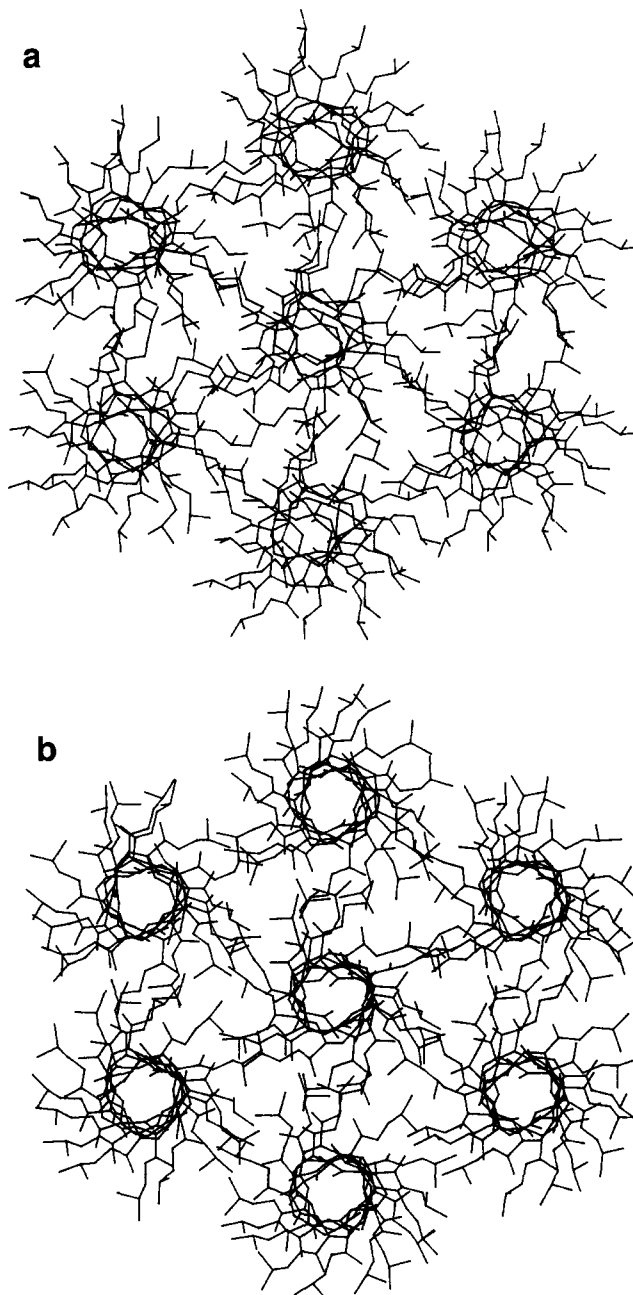


Figure 3 Minimized energy conformations of models (a) **1L** and (b) **2R**, with $\epsilon=1r$, viewed along the chain axis. The different aspect of the main chain results from a better hydrogen-bonding geometry in the model **2R**

interactions are taken into account, whereas a deviation of 15° is obtained when a unique chain is considered.

The total energy contributions indicate that model **2R** is approximately 20 kcal mol⁻¹ residue more favourable with respect to model **1L**. Electrostatic, van der Waals and bonding energetic contributions favoured the model **2R** by around 6 kcal mol⁻¹ residue each, for both dielectric constants. Model **2R** preserves better the average hydrogen-bonding geometry than model **1L**, as we see in Figure 3: the helices in model **1L** clearly appear more distorted at the main chain. Furthermore, the similarities between the model **2R** of the hexagonal form and the right-handed helix of the tetragonal form allow us to explain some experimental observations, e.g. that the transition between the hexagonal and tetragonal forms takes place easily², and that both forms have very similar n.m.r. spectra in the solid state¹⁹.

‡ The different energy terms refer to the middle residue of the central polymer chain, where both interresidue and intraresidue interactions were taken into account

Table 1 Results obtained from the energy minimization of models **1L** and **2R** using the two different expressions for the dielectric constant

Model ^a	Dielectric constant	Conformational angles (°)										Calculated energies (kcal mol ⁻¹ residue)						
		ϕ	ξ	ψ	ω	χ_1	χ_2	χ_3	χ_4	Dielectric constant	Contribution ^c	E_{bond}	E_{vdW}	E_{el}	E_{hb}	E_{tot}		
1L	1	149.5	-93.0	89.6	175.0	179.7	-170.4	-71.8	138.5	1	Intra	14.88	7.37	-124.63	-0.42	-102.81		
	1r	161.7	-96.8	74.7	-177.2	174.4	185.6	-68.8	144.7		Inter	3.56	-3.53	-73.65	-1.07	-101.68		
	LALS ^b	126.6	-102.8	113.6	180.0	175.0	180.0	-101.2	114.1		Total	18.44	-23.16	-198.29	-1.49	-204.49		
2R	1	157.2	-54.1	114.8	175.0	173.4	172.4	-108.1	112.7	1	Intra	10.99	6.54	-111.48	-0.48	-94.43		
	1r	149.6	-54.0	120.8	177.9	177.2	169.0	-101.1	107.2		Inter	1.49	-36.45	-94.02	-1.19	-130.17		
	LALS	145.2	-62.0	130.8	180.0	175.0	180.0	-101.2	114.1		Total	12.48	-29.91	-205.50	-1.67	-224.60		
											Intra	11.37	4.63	-29.63	-0.46	-14.09		
											Inter	0.80	-35.12	-52.32	-0.76	-87.40		
											Total	12.17	-30.48	-81.96	-1.23	-101.50		

^a Models **1L** and **2R** refer to a left-handed and a right-handed helix, respectively, with the hydrogen-bonding schemes **1** and **2** shown in Figure 2. The conformational angles correspond to those indicated in Figure 2 of ref. 4. The values given are the averages of the middle seven residues of the central chain

^b LALS-refined⁴ values are shown for comparison

^c The different energy terms refer to one residue, where E_{bond} = bonding energy, E_{vdW} = van der Waals energy, E_{el} = electrostatic energy, E_{hb} = energy corresponding to the $r^{-12} - r^{-10}$ term and E_{tot} = total energy. Inter and intra refer to interresidue and intraresidue energies; there is no distinction between intrahelical and interhelical interactions. The starting conformations were calculated with the LALS program taking into account the X-ray results⁴

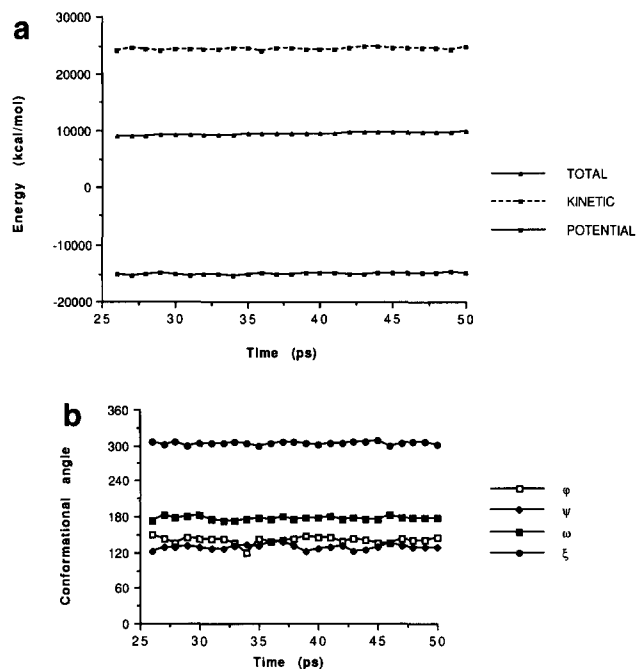

Figure 4 (a) Energy and (b) backbone conformational angle fluctuations along the last 25 ps of the molecular dynamics trajectory

Table 2 Averaged side-chain conformational angles and standard deviations (in parentheses) for the seven central residues along the last 25 ps of the trajectory. The total average values are also displayed for comparison with the LALS values (see Table 1)

Residue	Conformational angles (°)			
	χ_1	χ_2	χ_3	χ_4
1	168.1 (14.7)	-177.7 (11.7)	-169.8 (16.6)	58.7 (8.7)
2	-169.8 (33.6)	-173.8 (17.7)	-158.1 (39.1)	178.2 (11.0)
3	134.2 (14.0)	-172.6 (15.0)	-75.9 (44.0)	-179.2 (9.0)
4	-136.1 (16.3)	-165.0 (14.3)	174.4 (19.8)	-64.8 (18.7)
5	-156.9 (19.8)	-171.9 (11.1)	-172.3 (20.3)	-62.3 (20.4)
6	-132.1 (12.5)	171.5 (12.9)	176.7 (12.3)	54.5 (10.1)
7	177.2 (20.3)	179.4 (12.7)	-173.2 (10.2)	59.6 (12.0)
Total average	-170.8	-173.3	-159.7	160.7

The energy-minimized coordinates of model **2R** were taken as the starting point of a molecular dynamics trajectory. Figure 4 shows the fluctuations of the total energy of the system and the backbone torsion angles. The simulation reproduces reasonably well the refined X-ray structure. There are no large fluctuations in the backbone torsion angles, indicating small deviations relative to the X-ray results. These represent a very satisfactory agreement considering that energetic simulations have been carried out without geometrical constraints on the atomic coordinates.

Table 2 displays the side-chain conformational angles and standard deviations along the molecular dynamics trajectory for the seven central residues. An overall picture shows that whereas backbone conformational angles are conserved at the same value for each residue

along the trajectory, the side-chain dihedral angles display some variations for each residue depending on the packing environment. The seven central residues show different conformational angles and, in general, standard deviations are small. The lowest standard deviations correspond as might be expected to the ester group (χ_2), which has a conformational angle of around 180° . The largest standard deviations computed along the trajectory indicate that χ_3 is the most flexible angle, whereas χ_1 and χ_4 display similar values. Both side-chain angles χ_1 and χ_3 display an extended conformation, with the exception of residue 3 for which χ_3 corresponds to a *gauche* conformation. On the other hand, the results indicate a *gauche* (residues 1, 4, 5, 6 and 7) or a *trans* (residues 2 and 3) conformation for the χ_4 angle, depending on the interactions with the neighbouring chains. Thus, it seems that the packing environment affects considerably the conformation at the end of the side chain. The totally average conformational angles show a close resemblance to the LALS values, indicating that although they are physically unreasonable, they provide a good average picture of the side-chain conformation.

In summary, model **2R** is the minimum energy structure for the hexagonal form of PAIBLA by around 20 kcal mol^{-1} residue. This energy gap between models **2R** and **1L** is conserved for the different expressions of the dielectric constant. On the other hand, the molecular dynamics simulation shows that side-chain groups have different conformations depending on the packing environment generated by the neighbouring chains. Although these results could not be considered quantitatively owing to the limited duration of the simulation and the packing approximations, they provide a qualitative picture of the situation of side-chain conformations in the hexagonal crystalline form.

The present study represents an improvement of our previous work⁴. The results suggest that the combination of force-field calculations and refined crystallographic data seems to be very promising in structure determination, particularly in polymer fibres where poor crystallographic data are obtained.

ACKNOWLEDGEMENTS

The authors are indebted to Drs F. J. Luque and M. Orozco for the computational facilities. We also thank Drs J. A. Subirana and X. de la Cruz for helpful discussions. C. A. is grateful to the Departament d'Ensenyament de la Generalitat de Catalunya for support. This work was supported in part by DGICYT grant PB91-0588.

REFERENCES

- 1 Fernández-Santín, J. M., Aymami, J., Rodríguez-Galan, A., Muñoz-Guerra, S. and Subirana, J. A. *Nature (London)* 1984, **20**, 62
- 2 Muñoz-Guerra, S., Fernández-Santín, J. M., Alegre, C. and Subirana, J. A. *Macromolecules* 1989, **22**, 1540
- 3 Fernández-Santín, J. M., Muñoz-Guerra, S., Rodríguez-Galan, A., Aymami, J., Lloveras, J., Subirana, J. A., Giralt, E. and Pttack, M. *Macromolecules* 1987, **20**, 62
- 4 Bella, J., Alemán, C., Alegre, C., Fernández-Santín, J. M. and Subirana, J. A. *Macromolecules* 1992, **25**, 5225
- 5 Campbell-Smith, P. J. and Arnott, S. *Acta Crystallogr., Sect. A* 1978, **34**, 3
- 6 Manning, M. C., Fernández-Santín, J. M., Puiggali, J., Subirana, J. A. and Woody, R. W. *Biophys. J.* 1989, **55**, 530
- 7 Alemán, C., Subirana, J. A. and Perez, J. J. *Biopolymers* 1992, **32**, 621
- 8 Liao, W.-B. and Boyd, R. *Macromolecules* 1990, **23**, 1531
- 9 Ferro, D. R., Brückner, S., Meille, S. V. and Ragazzi, M. *Macromolecules* 1990, **23**, 1676
- 10 Ferro, D. R., Brückner, S., Meille, S. V. and Ragazzi, M. *Macromolecules* 1991, **24**, 1156
- 11 Alemán, C. and Perez, J. J. *J. Computer-Aided Mol. Design* 1993, **7**, 241
- 12 Alemán, C. and Perez, J. J. *J. Mol. Struct.* 1994, **304**, 17
- 13 Weiner, S. J., Kollman, P. A., Nguyen, D. T. and Case, D. A. *J. Comp. Chem.* 1986, **5**, 277
- 14 Weiner, S. J., Kollman, P. A., Case, D. A., Singh, U. C., Ghio, C., Alagona, G. and Weiner, P. *J. Am. Chem. Soc.* 1984, **106**, 765
- 15 Singh, U. C., Weiner, P. K., Caldwell, J. and Kollman, P. A. AMBER 3.0 Rev. A, 1989
- 16 Alemán, C., Canela, E. I., Franco, R. and Orozco, M. *J. Comp. Chem.* 1991, **12**, 664
- 17 Alemán, C. and Orozco, M. *J. Computer-Aided Mol. Design* 1992, **6**, 331
- 18 Goodfellow, J. M. *Mol. Sim.* 1990, **5**, 277
- 19 Quintero-Arcaya, R. A., Bovey, F. A., Fernández-Santín, J. M. and Subirana, J. A. *Macromolecules* 1990, **23**, 1531